Asian Journal of Chemistry; Vol. 25, No. 3 (2013), 1593-1596

ASIAN JOURNAL OF CHEMISTRY

http://dx.doi.org/10.14233/ajchem.2013.13354

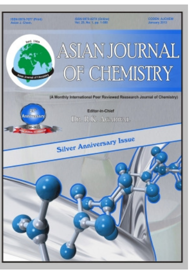

Influence of Hydrothermal Synthesis Condition on Structure and Microwave Properties of $Sr_{n+1}Ti_nO_{3n+1}$ Ceramics

HUANG ZHOU, JIANGYING WANG*, JINTAO LIU, SHENGYONG JIN and JINGJI ZHANG

College of Materials Science and Engineering, China Jiliang University, Hangzhou 310018, P.R. China

*Corresponding author: Tel.: +86 571 86875609; E-mail: wjyliu@163.com; zjjtongji@gmail.com

(*Received*: 29 December 2011; *Accepted*: 24 September 2012) AJC-12168

$Sr_{n+1}Ti_nO_{3n+1}$ (n = 1, 2) ceramics were prepared by using hydrothermal synthesis derived powders and the influence of hydrothermal synthesis condition on microwave properties were investigated. The hydrothermally synthesized powders mainly form $SrTiO_3$ and $Sr(OH)_2·mH_2O$. Grain size of the $SrTiO_3$ decreases with increasing the concentration of KOH and reaction temperature, which lend itself to the formation of $Sr_{n+1}Ti_nO_{3n+1}$ during sintering. $Sr_{n+1}Ti_nO_{3n+1}$ ceramics prepared by using high concentration of KOH have lower permittivity and higher Q value, due to the formation of pure phase $Sr_{n+1}Ti_nO_{3n+1}$ and low porosity of ceramics.

Key Words: Crystal structure, Hydrothermal crystal growth, Titanium compounds, Dielectric materials.

INTRODUCTION

Additions of excess SrO to $SrTiO_3$ form a homologous series with the general formula $Sr_{n+1}Ti_nO_{3n+1}$ (n = integer), which are known as Ruddlesden-Popper phase[1,2]. Its structure is composed of n $SrTiO_3$ perovskite-like layers sandwiched between SrO rock salt-type layers. The upper member of $Sr_{n+1}Ti_nO_{3n+1}$ is the well-known $SrTiO_3$ ($n = \infty$), whose electrical behaviour goes from a dielectric tunable property in its undoped form to a superconducting property when doped with a variety of elements[3]. It has been commonly used in grain boundary barrier-layer capacitors[4], resistive oxygen gas-sensors[5], solar cells[6], solid oxide electronic devices[7,8], *etc*.

This broad range of physical properties and applications of $SrTiO_3$ urges researchers to investigate physical properties of other members of $Sr_{n+1}Ti_nO_{3n+1}$. The ability to control permittivity and loss by varying *n* makes $Sr_{n+1}Ti_nO_{3n+1}$ candidate for microwave resonators[9]. Its relative permittivity decreases as n decreases. Sr_2TiO_4 (n = 1) and $Sr_3Ti_2O_7$ (n = 2) exhibit lower dielectric loss than $SrTiO_3$[9]. Unfortunately, it is difficult to form a single-phase $Sr_{n+1}Ti_nO_{3n+1}$ besides $SrTiO_3$, due to the phase transitions and decompositions[10]. The preparing methods of $Sr_{n+1}Ti_nO_{3n+1}$ ceramics are presently solid-phase reaction[9], mechanochemical activation process[11,12], molten salt synthesis[13] and sol-gel method[14]. From the view of synthesis, hydrothermal synthesis offers some advantages over the above methods, such as simplicity, relatively low reaction temperature and the capability to control crystal growth. No one has reported the hydrothermal synthesis of $Sr_{n+1}Ti_nO_{3n+1}$ so far.

Therefore, this study is focused on the influence of hydrothermal synthesis condition on structure and microwave properties of $Sr_{n+1}Ti_nO_{3n+1}$ (n = 1, 2) ceramics. More precisely, the hydrothermal reaction temperature and concentration of KOH were investigated to obtain pure phase $Sr_{n+1}Ti_nO_{3n+1}$ (n=1, 2). In addition, the structure evolution and reaction mechanism under certain circumstances were discussed.

EXPERIMENTAL

All the reagents were of analytical grade (Sinopharm Chemical Reagent Co., Ltd, China) and used as-received without further purification. The hydrothermal process was used for synthesizing $Sr_{n+1}Ti_nO_{3n+1}$ (n = 1, 2) from the following starting materials: $Sr(NO_3)_2$ (99.5 %), ($C_{16}H_{36}O_4Ti$) (98 %), ($C_5H_8O_2$) (99 %) and KOH (85 %). 0.03 mol of ($C_{16}H_{36}O_4Ti$) was mixed with 0.06 mol of ($C_5H_8O_2$) to form a yellowish solution. Meanwhile, 0.06 mol or 0.045 mol of $Sr(NO_3)_2$ was dissolved in 30 mL deionized water with the stoichiometric Sr/Ti molar ratio of 2.0 or 1.5, respectively. The above two solutions were mixed to form Sr-Ti solution. With stirring, 50 mL of 3.6 M or 100 mL of 15 M KOH solution was slowly added to the previously prepared Sr-Ti mixture with agitation, respectively. The precursors was transferred into a 200 mL Teflon-lined stainless steel reactor, sealed and then heated for 24 h at 180-210 ºC. After reaction, the autoclave was allowed to cool down room temperature. The as-synthesized powders were filtrated and washed with deionized water and ethanol to remove the remaining ions and then dried at 100 ºC for 6 h.

After drying, the powders were annealed at 800 °C for 4 h. The annealed powders, mixed with 8 wt % polyvinyl alcohol (PVA), were pressed into pellets at 100 MPa. The green pellets were kept at 550 °C for 6 h to remove the solvent as well as the binder and then sintered at 1450 °C for 4 h in air.

Crystalline phases were identified by means of X-ray diffraction (XRD, Bruker D_8 advanced, Germany) with CuK_α radiation. Microstructural information was obtained by using a scanning electron microscopy (SEM, JSM EMP-800). Permittivity and loss tangent at microwave frequencies were measured by the Hakki-Coleman dielectric resonator method, using a network analyzer (AV 3629A) in combination with a resonating cavity[15].

RESULTS AND DISCUSSION

Fig. 1 shows XRD patterns of the hydrothermally synthesized $Sr_{n+1}Ti_nO_{3n+1}$ (n = 1, 2) powders at 180 °C and 210 °C for 24 h with 3.6 M KOH, respectively. It can be seen that it does not depend on the hydrothermal reaction temperature whether it is 180 °C or 210 °C, $SrTiO_3$ is formed in all samples. At 180 °C, some additional peaks exist, which can be attributed to polycrystalline $Sr(OH)_2$ (JCPDS No. 74-1491). Its intensity becomes weaker with decreasing the molar ratio from 2 to 1.5, as shown in Fig. 1(a) and (b). When at 210 °C, additional low intensity reflection lines can be assigned to $Sr(OH)_2{\cdot}8H_2O$ according to JCPDS No. 73-2138, whose intensity also becomes weaker with decreasing the molar ratio [Fig. 1(c) and (d)]. The composition of synthesized powders at 180 °C for 24 h with 3.6 M and 15 M KOH has been also studied. There is no noticeable change in phase composition (no shown here).

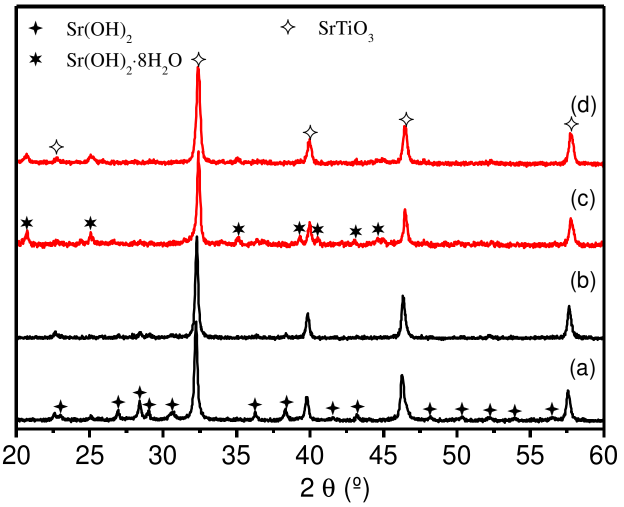

Fig. 1. XRD patterns of the hydrothermally synthesized $Sr_{n+1}Ti_nO_{3n+1}$ (n = 1, 2) powders at 180 °C [(a) n = 1 and (b) n = 2] and 210 °C [(c) n = 1 and (d) n = 2] for 24 h with 3.6 M KOH, respectively

To study its structure evolution with temperature, the $Sr_{n+1}Ti_nO_{3n+1}$ (n = 1, 2) powders synthesized at 210 °C for 24 h with 3.6 M KOH were annealed at 800 °C for 4 h and then sintered at 1450 °C for 4 h (Fig. 2). After annealing at the temperature of 800 °C, the $Sr(OH)_2{\cdot}mH_2O$ diffraction lines disappear and the $SrCO_3$ diffraction lines clearly appear. In addition, for the sample with n = 1, the $SrTiO_3$ diffraction peaks become weaker and the Sr_2TiO_4 diffraction lines also appear. Whereas for the sample with n = 2, no $Sr_{n+1}Ti_nO_{3n+1}$ phase is observed, the perovskite $SrTiO_3$ remaining unchanged. After sintering, it is interesting to observe that there is only Sr_2TiO_4 phase (according to JCPDS No. 72-2040 and 72-2041) in the sample with n = 1. Nevertheless, two phases corresponding to $Sr_3Ti_2O_7$ (JCPDS No. 76-0740) and $SrTiO_3$ are observable for the sample with n = 2.

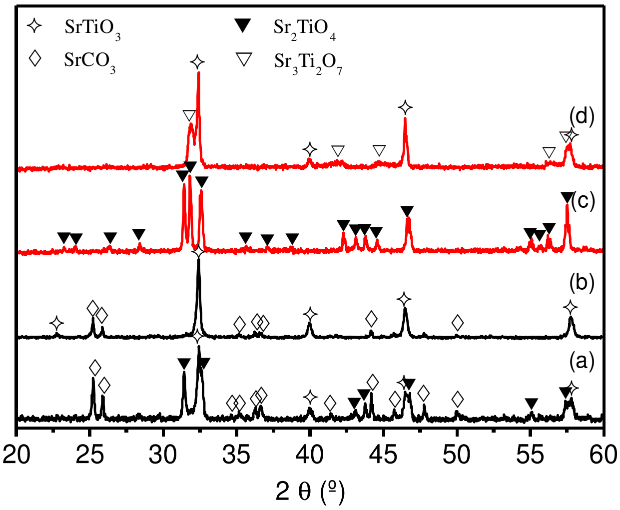

Fig. 2. XRD patterns of the $Sr_{n+1}Ti_nO_{3n+1}$ (n = 1, 2) annealed powders at 800 °C for 4 h [(a) n = 1 and (b) n = 2] and its corresponding sintered ceramics at 1450 °C for 4 h [(c) n=1 and (d) n=2] (the powders were hydrothermally synthesized at 210 °C for 24 h with 3.6 M KOH)

XRD patterns of the $Sr_{n+1}Ti_nO_{3n+1}$ (n = 1, 2) ceramics prepared by using hydrothermal reaction derived powders at 180 °C for 24 h with different concentration of KOH are given in Fig. 3. When $Sr_{n+1}Ti_nO_{3n+1}$ ceramics are prepared by using low concentration of KOH (3.6 M), Sr_2TiO_4 could be isolated as single phases for the sample with n = 1. However, for the sample with n = 2, there exist $Sr_4Ti_3O_{10}$ phase (JCPDS No. 76-0741) besides $SrTiO_3$ major phase. When $Sr_{n+1}Ti_nO_{3n+1}$ ceramics are prepared by using high concentration of KOH (15 M), Sr_2TiO_4 and $Sr_3Ti_2O_7$ are single phases for the samples with n=1 and 2, respectively. There is some disagreement about which phases are stable and which are metastable[3]. According to McCoy *et al.*, $Sr_3Ti_2O_7$ and $SrTiO_3$ are the only stable $Sr_{n+1}Ti_nO_{3n+1}$ phase. Additional stable Sr_2TiO_4 phase was also reported by Noguera. Obviously, Sr_2TiO_4 and $SrTiO_3$ phases are easily formed in our samples.

Based on the above results, several processes are taking place during both hydrothermal synthesis and heat treatments, so that the chemical reactions can be understood as follows:

$$(n+1)Sr^{2+} + nTi^{4+} \xrightarrow{\text{hydrotherm}\,(180^{o}C-210^{o}C)} SrTiO_3 + Sr(OH)_2 \cdot mH_2O$$

$$SrTiO_3 + Sr(OH)_2 \cdot mH_2O \xrightarrow{800^{o}C} SrTiO_3 + SrCO_3 + Sr_{n+1}Ti_nO_{3n+1}$$

$$SrTiO_3 + SrCO_3 + Sr_{n+1}Ti_nO_{3n+1} \xrightarrow{1450^{o}C} SrTiO_3 + Sr_{n+1}Ti_nO_{3n+1} + CO_2$$

The hydrothermally synthesized powders mainly form $SrTiO_3$ and $Sr(OH)_2{\cdot}mH_2O$ instead of $Sr_{n+1}Ti_nO_{3n+1}$ and the m value increases with respect to the reaction temperature.

In order to understand its structure evolution and reaction mechanism, grain size of the $SrTiO_3$ are calculated by using Debye-Scherrer formula: $D = 0.89\lambda/(\beta{\cdot}\cos\theta)$, where λ is the wavelength of the incident X-ray beam and β is the full width at half maximum of the XRD peak. (110) Diffraction peaks of $SrTiO_3$ are used to calculate grain size of $SrTiO_3$ and its grain sizes are listen in Table-1. It is notable that grain size decreases with increasing the concentration of KOH and reaction temperature. Similar result was ever reported by Lee *et al.*[16] that the crystallinity of $BaTiO_3$ powders prepared at low [KOH]/[Ti-isopropoxide] was substantially greater than that at high [KOH]/[Ti-isopropoxide]. During the heat treatment, the smaller the grain size of $SrTiO_3$ is, the more easily the $Sr_{n+1}Ti_nO_{3n+1}$ phase may form.

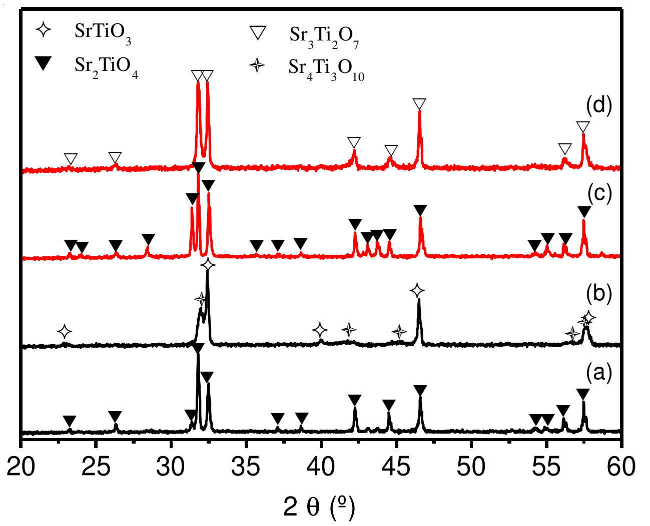

Fig. 3. XRD patterns of the $Sr_{n+1}Ti_nO_{3n+1}$ (n = 1, 2) ceramics prepared by using hydrothermal reaction derived powders at 180 ºC for 24 h with different concentration of KOH: (a) n = 1 with 3.6 M, (b) n = 2 with 3.6 M, (c) n = 1 with 15 M and (d) n = 2 with 15 M

TABLE-1
CALCULATED GRAIN SIZE OF THE $SrTiO_3$ IN THE $Sr_{n+1}Ti_nO_{3n+1}$ (n = 1, 2) SAMPLES SYNTHESIZED BY HYDROTHERMAL REACTION FOR 24 h WITH DIFFERENT CONCENTRATION OF KOH AND REACTION TEMPERATURE

Samples	KOH concentration	Hydrothermal temperature (ºC)	Grain size (nm)
n=1	3.6 M	180	30.0
n=2		180	32.5
n=1		210	31.0
n=2		210	26.4
n=1	15 M	180	22.6
n=2		180	18.1

The morphological characteristics of $Sr_{n+1}Ti_nO_{3n+1}$ (n = 1, 2) ceramics prepared by using hydrothermal reaction derived powders at 180 ºC for 24 h with different concentration of KOH were investigated by SEM (Fig. 4). It can be seen that there are a few pores in samples due to the decomposition of $SrCO_3$. For the n = 1 ceramics, the grain size decreases and its microstructure becomes homogeneous and dense with increasing the concentration of KOH, owing to the decreased grain size of $SrTiO_3$ derived by hydrothermal reaction. Whereas the n = 2 ceramics prepared with high concentration of KOH has a bimodal microstructure, consisting of pellet-shaped grains with size of 5-10 μm and fine grains of -1 μm. In addition, porous microstructure are also observed because the migration of grain boundaries is hindered during sintering[17].

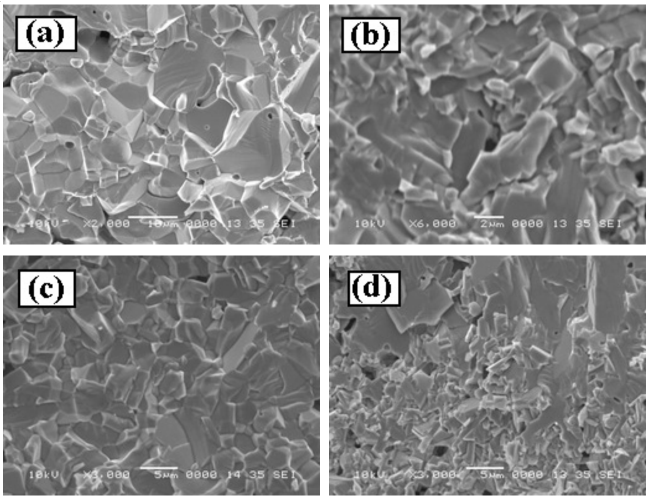

Fig. 4. Cross-section SEM images of the $Sr_{n+1}Ti_nO_{3n+1}$ (n = 1, 2) ceramics prepared by using hydrothermal reaction derived powders at 180 ºC for 24 h with different concentration of KOH: (a) n = 1 with 3.6 M, (b) n = 2 with 3.6 M, (c) n = 1 with 15 M and (d) n = 2 with 15 M

Microwave parameters of the $Sr_{n+1}Ti_nO_{3n+1}$ (n = 1, 2) ceramics prepared by using hydrothermal reaction derived powders at 180 ºC for 24 h with different concentration of KOH are measured at room temperature. Its permittivity and Q value are listed in Table-2. Permittivity of the $Sr_{n+1}Ti_nO_{3n+1}$ markedly increases with increasing n, whereas Q value markedly decreases. Moreover, it is interesting to observe that permittivity of $Sr_{n+1}Ti_nO_{3n+1}$ decreases with increasing the concentration of KOH, whereas Q value markedly increases. Structurally, permittivity and Q value depend on its composition and crystal structure. For the $Sr_{n+1}Ti_nO_{3n+1}$ ceramics prepared with high concentration of KOH, the low permittivity and high Q value is due to pure phase. It is of great interest that the Q value of $Sr_{n+1}Ti_nO_{3n+1}$ ceramics prepared by using hydrothermal synthesis derived powders is much higher than that prepared by solid state reaction[9].

TABLE-2
MICROWAVE PROPERTIES OF THE $Sr_{n+1}Ti_nO_{3n+1}$ (n=1, 2) CERAMICS PREPARED BY USING HYDROTHERMAL REACTION DERIVED POWDERS AT 180ºC FOR 24 h WITH DIFFERENT CONCENTRATION OF KOH

Samples	KOH concentration	Resonant frequency (GHz)	$ε_r$	Q value
n = 1	3.6M	6.316	46.5	6683
n = 2		4.128	99.3	4092
n = 1	15M	7.551	40.0	35194
n = 2		5.135	65.3	20402

Conclusion

Structural evolution and microwave properties analysis have been performed for $Sr_{n+1}Ti_nO_{3n+1}$ (n = 1, 2) ceramics prepared by using hydrothermal synthesis derived powders. The hydrothermally synthesized powders mainly form $SrTiO_3$ and $Sr(OH)_2{\cdot}mH_2O$ phases and the m value increases with respect to the reaction temperature. As the concentration of KOH and reaction temperature increases, the grain size of $SrTiO_3$ decreases. As a result, the small $SrTiO_3$ grains easily promote the formation of $Sr_{n+1}Ti_nO_{3n+1}$ phase during sintering. Especially, the $Sr_{n+1}Ti_nO_{3n+1}$ ceramics prepared with high concentration of KOH have pure phase $Sr_{n+1}Ti_nO_{3n+1}$ and dense microstructure, thus resulting in low permittivity and high Q value.

ACKNOWLEDGEMENTS

This research was supported by Zhejiang Provincial Science Foundation (No. Y6110475), the Research Fund for higher Education of Zhejiang Province (No. 01101158) and the undergraduate innovative project of Zhejiang Province (No. 2010R409016).

REFERENCES

1. S. Ruddlesden and P. Popper, *Acta Crystallogr.*, **10**, 538 (1957).
2. S. Ruddlesden and P. Popper, *Acta Crystallogr.*, **11**, 54 (1958).
3. J. Haeni, *Appl. Phys. Lett.*, **78**, 3292 (2001).
4. P. Balaya, M. Ahrens, L. Kienle, J. Maier, B. Rahmati, S.B. Lee, W. Sigle, A. Pashkin, C. Kuntscher and M. Dressel, *J. Am. Ceram. Soc.*, **89**, 2804 (2006).
5. Y. Hu, O. Tan, J. Pan, H. Huang and W. Cao, *Sensor. Actuat. B: Chem.*, **108**, 244 (2005).
6. S. Burnside, J.E. Moser, K. Brooks, M. Grätzel and D. Cahen, *J. Phys. Chem. B,* **103**, 9328 (1999).
7. J. Li, S. Luo and M. Alim, *Mater. Lett.*, **60**, 720 (2006).
8. J. Mateu, J.C. Booth and S.A. Schima, *IEEE Trans. Microw. Theory Tech.,* **55**, 391 (2007).
9. P. Wise, I. Reaney, W. Lee, T. Price, D. Iddles and D. Cannell, *J. Eur. Ceram. Soc.*, **21**, 1723 (2001).
10. E. Gutmann, A.A. Levin, M. Reibold, J. Muller, P. Paufler and D.C. Meyer, *J. Solid State Chem.*, **179**, 1864 (2006).
11. T. Hungria, A.B. Hungria and A. Castro, *J. Solid State Chem.*, **177**, 1559 (2004).
12. T. Hungria, I. MacLaren, H. Fuess, J. Galy and A. Castro, *Mater. Lett.*, **62**, 3095 (2008).
13. Y. Liu, Y. Lu, M. Xu and L. Zhoun, *J. Am. Ceram. Soc.*, **90**, 1774 (2007).
14. N. Zhou, G. Chen, H. Xian and H. Zhang, Mater. Res. Bull. 43 2554 (2008).
15. B.W. Hakki and P.D. Coleman, *IRE Trans. Microwave Theory Tech.*, **8**, 402 (1960).
16. S.K. Lee, G.J. Choi, U.Y. Hwang, K.K. Koo and T.J. Park, *Mater. Lett.*, **57**, 2201 (2003).
17. X. Wang, H.L.W. Chan and C.L. Choy, *J. Am. Ceram. Soc.*, **86**, 1809 (2003).